3D BIOPRINTING OF SCAFFOLD STRUCTURE USING MICRO-EXTRUSION TECHNOLOGY

Juan Xing, Xianli Luo, Juliana Bermudez, Matthew Moldthan, and Bingbing Li*

Department of Manufacturing Systems Engineering and Management, California State University, Northridge, CA 91330-8332

Abstract

Scaffold-based techniques are a vital assistance tool to support main structure and enhance the resolution of target structure. In this study, a custom-made micro-extrusion bioprinting system was built and utilized to fabricate different scaffold structures such as log-pile scaffold and two-ring scaffold. This approach showed tremendous potential because of its ability to produce microscale channels with almost any shape. We were able to fabricate these scaffolds by using a custom-made 3D bioprinter to print hydrogel solution, mostly composed of Pluronic F-127, then wash away hydrogen by phosphate buffer saline (PBS) after crosslinking of main structure. We were able to achieve the desired scaffold structure by feeding G-codes data into user interface (Pronterface) and then translating that model into a program that utilizes a customized programming language, which instructs the microfabrication printer nozzles to dispense the hydrogel at specific locations. This fundamental study will be used to print increasingly viable and complex tissue shapes with living cells.

1. Introduction

One of the foremost challenges facing scientists and researchers today in the field of three-dimensional (3D) bioprinting is the formation of viable and structurally sound tissues and organs. The ever-growing demand for tissue and organ transplants has driven researchers to develop several different approaches to address this challenge. 3D bioprinting has opened the doors to new methods of printing, especially the methods used for tissue engineering and the production of artificial organs and tissues[1]. Having the capability to 3D print functional artificial tissues on demand is extremely beneficial for studying all aspects of these tissues and organs which may ultimately eliminate the need for donors[2]. Scaffold-based techniques provide an ideal support for cell adhesion, proliferation, distribution, and invasion[3]. The structure of the scaffold can be modulated in order to re-create biological environments by arranging the scaffold's spatial organizations that may be similar to in vivo tissues or organs[4].

Additionally, various formats and modifications to scaffold models, with respect to the choice of biomaterials and physical conditions, have been implemented to optimize the growth of cancer cells on a scaffold[5]. It provides a way to mimic a natural tumor microenvironment which has become an approach to understanding cancer, while taking an insight into the potential motility of cancer cells in human bodies.

A log-pile scaffolds is often used in cancer study for cell transmigration, where the spacing between the lines is based on the typical size of a cancer cell[6]. The biggest challenge for 3D log-pile scaffold is to obtain high resolution, which is dependent of the width of the logs and the distance between the logs. For printing tissues and organs, the higher resolution of printed

logs, the more sophisticated scaffold structure will be achieved. For the motility of cancer cells, they need micro-channels otherwise they tend to drop down to the bottom in the scaffold.

In this study, a custom-made micro-extrusion bioprinting system was built and utilized for printing biological structures. This inexpensive method can be used to print desired shapes, and has flexibility in the selection of the hydrogels used[7]. The bio-ink used is comprised of Pluronic F127 and glycerol, which was printed in a petri dish and maintained in room temperature before being used. Pluronic F127 with low biological toxicity and biocompatibility, has been a great candidate for cell encapsulation applications, either by itself or to specifically promote cell seeding and attachment in tissue scaffolds[8]. Glycerol, on the other hand, was used because of its well-known osmotic stabilizing properties[9]. As a result, Glycerol acts as lubricating agent to prevent clogging in micro-needles since glycerol can protect the bacteria against excessive stress caused by the encapsulation procedure. In order to obtain an optimal scaffold structure, we optimized parameters of the custom-made printing system, including needle diameter, interval between lines, extruding distances of piston for log and turning point, and extruding speed. Hydrogel preparation, bioprinting system setup, results and discussion will be presented in the following sessions.

2. Hydrogel Preparation

All solutions were prepared as a percent by mass. In a mason jar, Pluronic F-127 (P2443; Sigma-Aldrich) and glycerol (Sigma-Aldrich) were mixed in distilled water, resulting in concentration of Pluronic F-127 (33% w/v) and glycerol (10% v/v). The starchy mixture was stored at 4°C for 3 hours to obtain a liquid solution. The aqueous transparent solution was stirred for 1 hour, then was stored at 4°C before use. The liquid state of the solution provides convenience of application when it is being poured into a 20ml syringe. The syringe is then left at room temperature to start the formation of the non-occlusive gel on warming. The thermal gelation of Pluronic F-127 allows for a rapid printing due to its increase in contact time which produces a stable structure[10]. After leaving the material at room temperature for one hour, the solution is ready to be used for printing.

Pluronic F127 aqueous solutions at 20 to 30% w/w has been known to having interesting characteristic of reverse thermal gelation[11]. Pluronic F-127 is at a liquid state when refrigerated at temperatures of 4-5°C, and gel upon warming to room temperature. The gelation is reversible upon cooling. The physical properties of this material makes it suitable to be used in micro-extrusion due to the ability to reverse thermal gelation. A hydration layer surrounds Pluronic F-127 molecules at its aqueous state. As the temperature raises, the hydrophilic chains inside the copolymer become desolated which enables a breakage of the hydrogen bonds established between the solvent and these chains[12]. This phenomenon leads to gel formation. This thermal reversible biopolymer gel has been widely used for pharmaceutical formulations and studies have demonstrated its high biocompatibility for biomedical applications, including grafts for wounds[13] and drug delivery[14-15].

3. Bioprinting System

The design of the models was manually done by using a featured G-code sender with a graphical user interface (Pronterface). The software has a printer control section, a print simulation, a G-code sender, and a command prompt. The printer control section allows for auto-

homing and moving of the axis. The print simulation area allows the user to see the design that will be printed based on the G-code made, and where in the platform. The G-code sender allows the user to directly send a G-code to the printer. The G-code, which provides existing standard protocols that can be easily modified, was manually written in order to control the intervals between the logs, the inner and outer diameter, as well as the supporting slopes. The G-code controls the tool pass and enables it to stop the process at each layer in order for solidification to occur.

The biological structure processing in the study was implemented by using a micro-extrusion method executed on a custom built XYZ stages attached to a lid-screw syringe-based assembly that was custom designed in Figure 1. The syringe extruder was design for enabling precise hydrogel deposition. All the parts to make the custom syringe were 3D printed by a Stratasys uPrint SE 3D Printer. The syringe-based extruder uses an individual stepper motor independent of the XYZ axis platform to slowly move the plunger from a 20 ml syringe at a resolution of 500 micron. Therefore, parameter modifications are needed to create a well-defined structure in terms of nozzle diameter, filament diameter, speed, flow, and G-code. A dispensing tip is used on the end of the syringe in order to control the volume of hydrogel being extruded. This method works by extruding a hydrogel material from the syringe to a petri dish. The petri dish was manually placed in the platform, while the extruder nozzle was positioned on top of the petri dish and the G-code of the desired design was sent to the printer. The printing process is set to slow in order to allow the solution to cool down and solidify on its own. When the printing process is concluded, the printed object is ready.

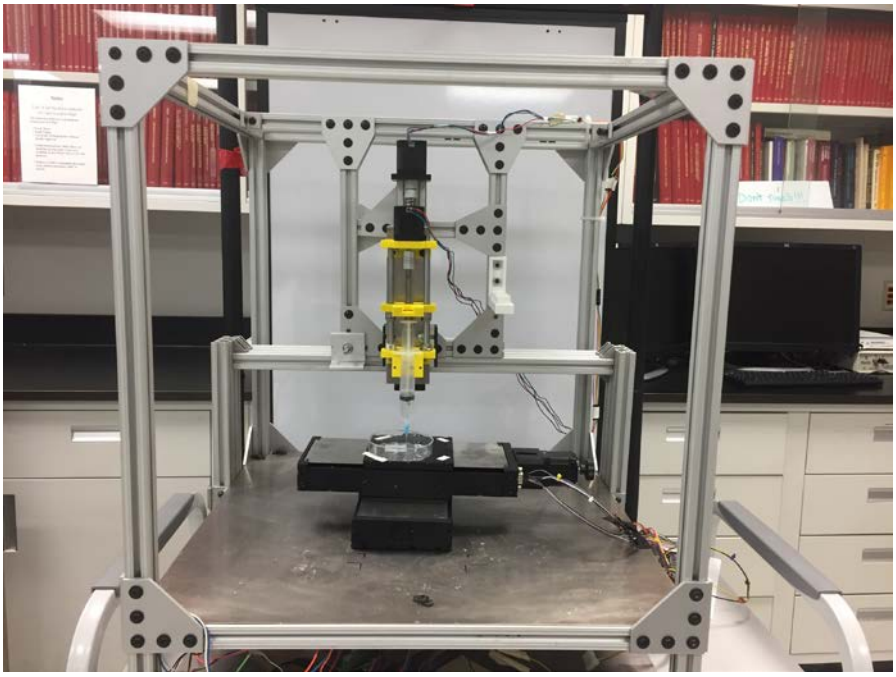

Figure 1 Micro-extrusion Bioprinting System.

4. Fabrication of Two scaffold modes

4.1 Mode 1: Fabrication of log-pile scaffold

Log-pile scaffolds are widely used in 3D bio-printing to fabricate artificial tissues and organs. Additionally, log-pile scaffolds enables to create a micro-environment so that it can be used to research the immigration path of cancer cells[15]. Therefore, in the both field of printing artificial tissues and organs, and exploring the metastatic path, log-pile scaffold plays a vital role.

Log-pile scaffolds consist of several layers of 2D slab, with a previously formed log oriented perpendicularly. Since the extruding process was continuous, the width of an extruded log was always larger at the cross-sections due to the surface tension. Before printing log-pile scaffold with our micro-extrusion bioprinting system, we carried out a set of adjustment for 2D slab. As long as we can get micron-scaled interval between logs, it will be easy to print sound log-pile scaffold with micro-channel.

Adjustment in Setting Parameters for 2D slab

In order to appropriately use the hydrogel solution on the printing systems there were various considerations that needed to be taken into account. We evaluated the hydrogel and bioprinting system based on five parameters that we believe would have an impact on the bioprinted structure. Specifically these are: distance from needle tip to plate surface (D, mm), moving distance of piston for one log (E1, mm), moving distance of piston for one turning short log (E2, mm), the speed of piston movement for one log (F1, mm/min), and the speed of piston movement for one turning short log (F2, mm/min). All the data was taken in millimeters or millimeters per minute for dimensions and velocity respectively. A collection of these parameters for the evaluated trials is shown in Table 1.

Table 1 Optimization of Printing Parameter

Trial ID	Needle Diameter (mm)	Interval between logs (mm)	D	E1	E2	F1	F2
1	0.7	2	1	0.1	0.1	400	400
2	0.5	1.5	1	0.07	0.07	400	400
3	0.5	1.2	0.8	0.05	0.05	400	400
4	0.5	1.2	0.5	0.05	0.05	400	400
5	0.5	1.2	0.5	0.05	0.03	400	400
6	0.5	1.2	0.5	0.03	0.03	400	400
7	0.5	1.0	0.5	0.02	0.02	400	300
8	0.5	1.0	0.3	0.02	0.02	400	300

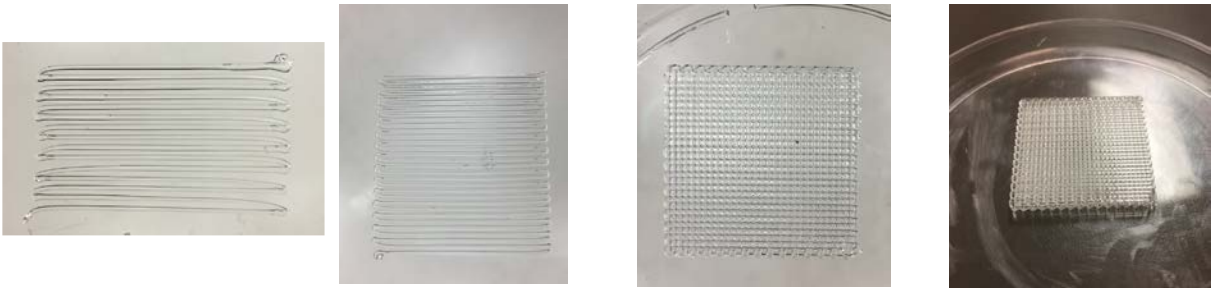

a **b** **c** **d**

Figure 2. Log-Pile Structure. (a) The structure (30mm*15mm) shows the optimal 2D slab with 0.5mm of log diameter and 0.5mm of interval. (b) The 2D slab was extended into a square slab (30mm*30mm). (d) A two-layer log-pile scaffold where second layer was rotated by 90°. (d) A six-layer log-pile scaffold (30mm*30mm*2mm) was built by repeating C for three times.

After the log-pile scaffold with 0.5mm of log diameter and 0.5mm of interval was successfully printed, we continued to reduce the micro-channels. In order to fabricate the log-pile scaffold with 0.5mm of log diameter and 0.3mm of interval, we adjusted the parameters. Based on several trials, the optimal parameters in settings were 0.3mm of the initial distance from needle tip to plate surface, 0.5mm of Interval between logs, 0.019mm of E1, 0.019mm of E2, 400mm/min of F1, and 300 mm/min of F2. The log-pile scaffold with smaller micro-channels was printed out with the parameters, was showed in Figure 3.

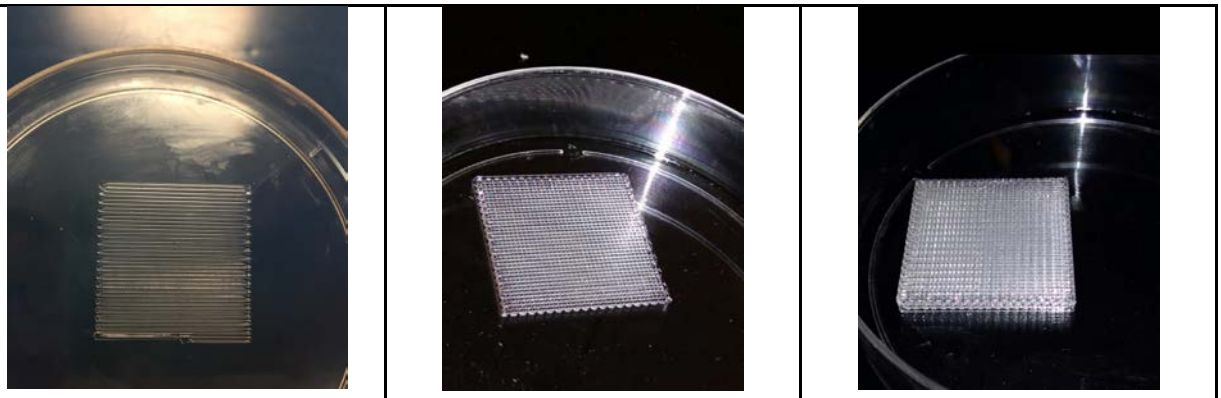

a	b	c

Figure 3. Log-Pile Structure. (a) The square structure (30.4mm*30.4mm) shows the optimal 2D slab with 0.5mm of log diameter and 0.3mm of interval. (b) A two-layer log-pile scaffold where second layer was rotated by 90°. (c) A six-layer log-pile scaffold (30.4mm*30.4mm*2mm) was built by repeating B for three times.

4.2 Mode 2: Fabrication of ring scaffolds

Vascular-like constructs have been successfully printed in many tissue engineering labs, and it is a common way to fabricate it in log-pile scaffold[16]. However, we have not seen any labs utilize ring scaffold. Saving scaffold material is one of the significant advantages for ring scaffold.

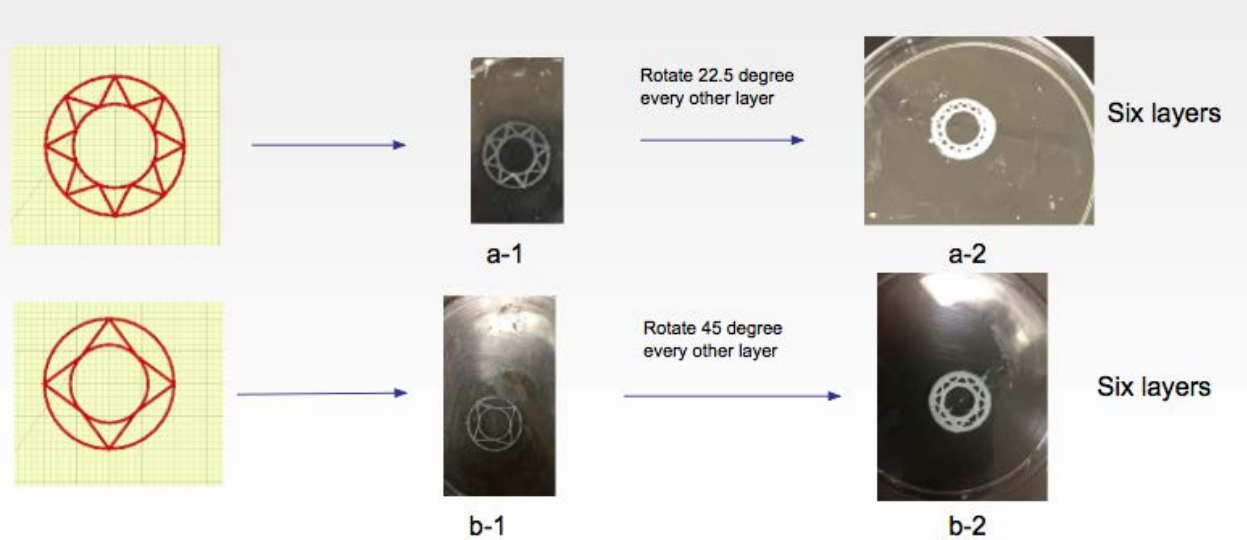

Figure 4. Ring Scaffolds. (a-1) The first layer of scaffold (a-2). The pattern was rotated by 22.5 degrees every other layer. (b-1) The first layer of scaffold (a-2). The pattern was rotated by 45 degrees every other layer.There were six layers in both scaffold a-2 and b-2.

We created two types of ring scaffold a-2, b-2 showed in Figure 4. These two have the same diameter of outer circle (20mm), same diameter of inner circle (12mm), same thickness (4mm), and the same height (2mm). The only difference is the number of crossed lines. Scaffold a-2 has twice number of zigzag lines as b-2, which results in different traits and functionalities. Scaffold a-2 can provide more support for main structure while Scaffold b-2 can create more space for the material of main structure.

5. Discussion

It is the crossed lines that enhances the stability of scaffold and creating support for main structure. For mode 1, log-pile scaffold, the 2D structure in Table 1 shows the process we reduced the log's diameter and intervals between two logs. The 2D structure in Figure 3 indicates the smallest interval between logs (300 microns) we can get so far with our micro-extrusion bioprinter. Based on one layer of paralleled logs we printed 6 layers logs-piled structure shown in Figure 2 and Figure 3. The even layers and odd layers were interleaved by 90°, forming a polyporous structure. For mode 2, ring scaffold, we created two different rings via designing different first layer and rotating the even layers by different degrees, showed in Figure 4. In mode 1 we used thinner needle with diameter of 0.5mm as there were so many thin logs crossed that the scaffold was stable enough. However thicker needle with diameter of 0.7mm was used in mode 2 since we need build thicker inner and outer wall for ring scaffold or it was likely to collapse.

In the parameter settings, D, E1, E2 were three critical parameters that needed to be iteratively adjusted. If D, distance from needle tip to plate surface, was too high, the part near turning section would become messy. If D was too low, the logs would become too thick, that was likely to reduce the interval space. E1 and E2 controlled the amount of extruded material for the log between two specific points, but the value of E1 and E2 were not proportional to the length of corresponding log due to the inertia effect of extrusion.

6. Conclusion and Future Work

In this study we optimized parameters of the custom-made printing system, including needle diameter, interval between lines, extruding distances of piston for log and turning point, and extruding speed. This fundamental study will be used to print increasingly viable and complex tissue shapes with living cells.

Future work may include the following: testing lower concentrations of bacterial cellulosic exopolysaccharide gel on this micro-extrusion bioprinter to test the compatibility; improve the XYZ stages and dispensing nozzle parameters and increase accuracy and transparency of alginate models; inclusion of cells in hydrogel to test cell viability.

7. Acknowledgements

This research work was supported by the NIH NIGMS BUILD (Building Infrastructure Leading to Diversity) PODER (Promoting Opportunities for Diversity in Education and Research) Faculty Scholar Academy and Mentor Training (1RL5GM118975), Equipment (8UL1GM118976) and Student (8TL4GM118977). It was also supported by the NSF CSU I-Corps Site (California State University Innovation Corps) Faculty Lead Microgrant (57866AP38147811213).

8. References

1. Ma, Z., Koo, S., Finnegan, M. A., Loskill, P., Huebsch, N., Marks, N. C., Conklin, B.R., Grigoropoulos, C. P., and Healy, K. E. (2014). Three-dimensional filamentous human diseased cardiac tissue model. *Biomaterials, 35*(5), 1367-1377.
2. Nunes, S. S., Miklas, J. W., Liu, J., Aschar-Sobbi, R., Xiao, Y., Zhang, B, Jiang, J., Masse, S., Gagliardi, M., Hsieh, A., Thavandiran, N., Laflamme, M. A., Nanthakumar, K., Gross, G. J., Backx, P. H., Keller, G., and Radisic, M. (2013). Biowire: A platform for maturation of human pluripotent stem cell-derived cardiomyocytes. *Nature Methods, 10*(8), 781-787.
3. Zhang, Y. S., and Xia, Y. (2015). Multiple facets for extracellular matrix mimicking in regenerative medicine. *10*(5), 689-692.
4. Zhang, Y. S., Arneri, A., Bersini, S., Shin, S. R., Zhu, K., Goli-Malekabadi, Z., Aleman, J., Colosi, C., Busignani, F., Dell'Erba, V., Bishop, C. Shupe, T., Demarchi, D., Moretti, M,. Rasponi, M., Dokmeci, M. R., Atala, A., Khademhosseini, A. (2016). Bioprinting 3D microfibrous scaffolds for engineering endothelialized myocardium and heart-on-a-chip. *Biomaterials, 110*, 45-59.
5. Rijal, G., and Li, W. M., (2016). 3D scaffolds in breast cancer research. *Biomaterials, 81*, 135-156.
6. Zhang L. G., Fisher, J. P., Leong, K. W. (2015). 3D Bioprinting and Nanotechnology in Tissue Engineering and Regenerative Medicine, *Elsevier,* 25-57.
7. Murphy, S. V., Atala A. (2014). 3D bioprinting of tissues and organs. *Nature Biotechnology, 32*(8), 773-85.
8. Diniz, I., Chen, C., Xu, X. T., Ansari, S., Zadeh, H., Marques, M., Shi, S. T., Moshaverinia, A. (2015). Pluronic F-127 hydrogel as a promising scaffold for encapsulation of dental-derived mesenchymal stem cells. *Journal of Materials Science: Materials in Medicine, 26*(3), 1-10.

9. Khattak, S. F., Bhatia, S. R, and Roberts, S. C, (2015) Pluronic F127 as a Cell Encapsulation Material: Utilization of Membrane-Stabilizing Agent, *Tissue Engineering,* 11(5-6): 974-983.
10. Kang, H. W., Lee S. J., Ko, I. P, Kengla, C., Yoo, J. J., and Atala, A. (2016). A 3D bioprinting system to produce human-scale tissue constructs with structural integrity. *Nature Biotechnology*, *34*(3), 312-319.
11. Miyazaki, S., Takeuchi, S., Yokouchi, C., Takada, M. (1984) Pluronic F-127 gels as vehicles for Topical administration of Anticancer Agents, *Chem. Pharm. Bull*., 32(10),4205-4208.
12. Escobar-Chávez, J. J., López-Cervantes, M., Naik, A., Kalia, Y., Quintanar-Guerrero, D., and Ganem-Quintanar, A. (2006). Applications of thermo-reversible pluronic F-127 gels in pharmaceutical formulations. *Journal of Pharmacy & Pharmaceutical Sciences, 9*(3), 339-58.
13. Nalbandian, R. M., Henry, R. L., Balko, K. W., Adams, D. V., and Neuman, N. R. (1987). Pluronic F-127 gel preparation as an artificial skin in the treatment of third-degree burns in pigs. *Journal of Biomedical Materials Research, 21*(9), 1135-48.
14. Bourre, L., Thibaut, S., Lajat, Y., Briffaud, A., Patrice, T. (2002) Potential efficacy of a delta 5-aminolevulinic acid thermosetting gel formulation for use in photodynamic therapy of lesions of gastrointestinal tract, *Pharmacological Research*, 45(2): 159-165.
15. Xia, W., Cao, Y., and Shang, Q. (2001) An experimental study of tissue engineered autologous cartilage by using an injectable polymer, *Chinese Journal of Plastic Surgery*, 17(5): 302-305.
16. Shan, J. N., Pan, C. C., Elomaa L., and Yang Y. A. (2015) Novel Bioprinting Method and System for Forming Hybrid Tissue Engineering Constructs. *Biofabrication.* 7(4): 045008.